A CASE STUDY OF INVERSE DYNAMICS CONTROL
OF MANIPULATORS WITH PASSIVE JOINTS

Wojciech Blajer, Krzysztof Kołodziejczyk

University of Technology and Humanities in Radom, Faculty of Mechanical Engineering, Radom, Poland
e-mail: w.blajer@uthrad.pl; k.kolodziejczyk@uthrad.pl

Manipulators with both active and passive joints are examples of underactuated systems, featured by less control inputs than degrees of freedom. Due to the underactuation, in the trajectory tracking (servo-constraint) problem, the feed-forward control obtained from an inverse model is influenced by internal dynamics of the system, leading to a more involved control design than in the fully actuated case. It is demonstrated that a convenient approach to the problem solution is to formulate the underactuated system dynamics in the input-output normal form, with the arising governing equations formulated either as ODEs (ordinary differential equations) or DAEs (differential-algebraic equations). The interrelationship between the inverse dynamics control and the associated internal dynamics is then studied and illustrated using a planar manipulator with two active and one passive joint. Some simulation results for the sample case study are reported.

Keywords: inverse dynamics, underactuated manipulators, passive joints, servo-constraints

1. Introduction

Most typically, manipulators are designed and modeled as fully actuated, in which the number m of control inputs equals the number f of degrees of freedom, $m = f$. Given a (fully) prescribed motion of the system, the inverse dynamics simulation allows for determination of the desired control, which, combined with feedback linearization, is used in the computed torque controllers (Paul, 1981). The situation is different for manipulators with elastic/passive joints and/or flexible members (Spong, 1987; De Luca and Oriolo, 2002; Benosman and Le Vey, 2004), where the related unactuated degrees of freedom result in underactuation of the system, $m < f$ (less control inputs than degrees of freedom). A desired motion of such systems can be partly prescribed by m outputs, whose number coincides with the number of inputs. The motion specifications lead to servo-constraints on the system (Kirgetov, 1967; Bajodah *et al.*, 2005; Blajer and Kołodziejczyk, 2007, 2008) with the system input control forces referred to as reactions of the constraints. The servo-constraint problem is then a specific inverse dynamics simulation problem in which the input control strategy that forces an underactuated system to complete the partly specified motion is to be determined.

The servo-constraint problem analyzed in the previous works (Blajer and Kołodziejczyk, 2007, 2008) addressed mainly the so-called differentially flat problems (Fliess *et al.*, 1995), in which all system states and control inputs can be expressed algebraically in terms of outputs and their time derivatives up to a certain order, with no internal/unspecified dynamics left in the system. The differential flatness for underactuated systems is also consequent to tangential or mixed orthogonal-tangential realization of the related servo-constraints. By contrast, the servo-constraint problem analyzed in this paper, for manipulators with both active (actuated) and passive (unactuated) joints, is a non-flat problem, and orthogonal realization of the related servo-constraints is observed. The orthogonal realization of servo-constraints means that the inverse dynamics control can be determined using an input-output normal form, which is then

associated with the internal dynamics. Due to a mutual relationship between the inverse control and internal dynamics, the problem becomes a dynamic problem, and stability of the internal dynamical is of crucial importance. As shown by Seifried (2012a), the stability can be achieved by a suitable manipulator design or, as motivated hereafter, by appropriate imposition of motion specifications. All these issues are addressed in the present paper, with a uniform formulation of the governing equations which arise either as ordinary differential equations (ODEs) or differential-algebraic equations (DAEs). The subject-specific stability problems are then illustrated using a planar manipulator with two (first) active and one (last) passive joints, $f = 3$ and $m = 2$. Some simulation results for the sample case study are also reported.

2.   Formulation of the problem

Let us consider an f-degree-of-freedom underactuated mechanical system, described by configuration coordinates $\mathbf{q} = [q_1, \ldots, q_f]^\mathrm{T}$, and controlled by m inputs $\mathbf{u} = [u_1, \ldots, u_m]^\mathrm{T}$, $m < f$. The nonlinear dynamic equations of the system are

$$\mathbf{M}(\mathbf{q})\ddot{\mathbf{q}} + \mathbf{k}(\mathbf{q}, \dot{\mathbf{q}}) = \mathbf{g}(\mathbf{q}, \dot{\mathbf{q}}) + \mathbf{B}(\mathbf{q})\mathbf{u} \tag{2.1}$$

where $\mathbf{M}$ is the $f \times f$ generalized mass matrix, $\mathbf{k}$ is the f-vector of dynamic terms, $\mathbf{g}$ is the f-vector of applied forces, and $\mathbf{B}$ is the $f \times m$ matrix of maximal column rank that projects the control inputs $\mathbf{u}$ on the directions of $\mathbf{q}$. The m system outputs $\mathbf{y} = [y_1, \ldots, y_m]^\mathrm{T}$ can be expressed in terms of $\mathbf{q}$, with the following relationships at the position, velocity and acceleration levels

$$\mathbf{y} = \boldsymbol{\Phi}(\mathbf{q}) \qquad \dot{\mathbf{y}} = \mathbf{H}(\mathbf{q})\dot{\mathbf{q}} \qquad \ddot{\mathbf{y}} = \mathbf{H}(\mathbf{q})\ddot{\mathbf{q}} + \mathbf{h}(\mathbf{q}, \dot{\mathbf{q}}) \tag{2.2}$$

where $\boldsymbol{\Phi} = [\Phi_1, \ldots, \Phi_m]^\mathrm{T}$ are appropriately differentiable functions of $\mathbf{q}$, the $m \times f$ Jacobian matrix $\mathbf{H} = \partial\boldsymbol{\Phi}/\partial\mathbf{q}$ is of maximal row rank, and the m-vector $\mathbf{h} = \dot{\mathbf{H}}\dot{\mathbf{q}}$ involves accelerations induced by the output relationship of Eq. (2.2)$_1$.

A desired/specified motion of an underactuated system can be given in time as $\mathbf{y} = \widetilde{\mathbf{y}}(t)$. The relationships of Eq. (2.2) lead then to *servo-constraints* on the system with the following equations at the position, velocity and acceleration levels

$$\boldsymbol{\varphi}(\mathbf{q}, t) = \boldsymbol{\Phi} - \widetilde{\mathbf{y}} = \mathbf{0} \qquad \boldsymbol{\gamma}(\dot{\mathbf{q}}, \mathbf{q}, t) = \mathbf{H}\dot{\mathbf{q}} - \dot{\widetilde{\mathbf{y}}} = \mathbf{0}$$
$$\boldsymbol{\eta}(\ddot{\mathbf{q}}, \dot{\mathbf{q}}, \mathbf{q}, t) = \mathbf{H}\ddot{\mathbf{q}} + \mathbf{h} - \ddot{\widetilde{\mathbf{y}}} = \mathbf{0} \tag{2.3}$$

The servo-constraints introduced in Eq. (2.3)$_1$ are mathematically equivalent to *passive* (or *contact*) constraints on the system, $\boldsymbol{\varphi}(\mathbf{q}, t) = \mathbf{0}$. By analogy to the constrained system dynamics, the generalized actuating force $\mathbf{g}_u = \mathbf{B}\mathbf{u}$ can be viewed as a generalized reaction force of the servo-constraints. There is, however, a substantial difference between the passive-constraint realization and the servo-constraint realization (Blajer and Kołodziejczyk, 2007, 2008). Whereas the generalized reaction of (ideal) passive constraints is by principle orthogonal to the passive constraint manifold, the generalized actuating force can be arbitraily oriented with respect to the servo-constraint manifold (it may also be tangent to the manifold). As it will be seen further, in the case of manipulators with passive joints, there is typically an explicit input-output relationship (the system outputs $\mathbf{y}$ are directly actuated by the inputs $\mathbf{u}$), which indicates an orthogonal realization of servo-constraints, and is conditioned upon the maximal rank of the $m \times m$ matrix $\mathbf{Y} = \mathbf{H}\mathbf{M}^{-1}\mathbf{B}$, $\mathrm{rank}(\mathbf{Y}) = m$ and $\det(\mathbf{Y}) \neq 0$; see also Blajer and Seifried (2012), Seifried (2012a,b), and Seifried and Blajer (2013), This is not, however, an ideal orthogonal realization, but a non-ideal orthogonal one, which denotes that the control required for the servo-constraint realization has an influence also on the internal (unspecified) dynamics of the system.

3. Governing equations

The servo-constraint problem can be formulated in different ways; see e.g. Spong (1998), Fantoni and Lozano (2002), Bajodah *et al.* (2005), Blajer and Kołodziejczyk (2007, 2008), and Seifried (2012b) for some of the possibilities. A convenient setting can be achieved by applying a coordinate transformation, from the configuration coordinates $\mathbf{q}$ to a new set of coordinates that include the system outputs $\mathbf{y}$. Motivated by a similar approach presented by e.g. Spong (1998) and Seifried (2012a,b), the f generalized coordinates $\mathbf{q}$ are first partitioned into m actuated and $f - m$ unactuated coordinates, written symbolically as $\mathbf{q} = [\,\mathbf{q}_a^{\mathrm{T}}\ \ \mathbf{q}_u^{\mathrm{T}}\,]^{\mathrm{T}}$, conditioned upon the $m \times m$ matrix $\mathbf{B}_a$, which gathers the rows of $\mathbf{B}$ related to $\mathbf{q}_a$, is of maximal rank, $\det(\mathbf{B}_a) \neq 0$. The partitioned forms of the output relationships introduced in Eqs. $(2.2)_{2,3}$ are then

$$\dot{\mathbf{y}} = \mathbf{H}_a \dot{\mathbf{q}}_a + \mathbf{H}_u \dot{\mathbf{q}}_u \qquad\qquad \ddot{\mathbf{y}} = \mathbf{H}_a \ddot{\mathbf{q}}_a + \mathbf{H}_u \ddot{\mathbf{q}}_u + \mathbf{h} \tag{3.1}$$

where $\mathbf{H} = [\,\mathbf{H}_a \,\vdots\, \mathbf{H}_u\,]$, and $\mathbf{H}_a$, $\mathbf{H}_u$ are of dimensions, respectively, $m \times m$ and $m \times (f - m)$.

The new set of coordinates is $\mathbf{q}' = [\,\mathbf{y}^{\mathrm{T}}\ \mathbf{q}_u^{\mathrm{T}}\,]^{\mathrm{T}}$, where, compared to $\mathbf{q} = [\,\mathbf{q}_a^{\mathrm{T}}\ \mathbf{q}_u^{\mathrm{T}}\,]^{\mathrm{T}}$, the outputs $\mathbf{y}$ are introduced instead of $\mathbf{q}_a$. At the acceleration level, the transformation formula is

$$\ddot{\mathbf{q}}' = \begin{bmatrix} \ddot{\mathbf{y}} \\ \ddot{\mathbf{q}}_u \end{bmatrix} = \begin{bmatrix} \mathbf{H}\ddot{\mathbf{q}} \\ \ddot{\mathbf{q}}_u \end{bmatrix} + \begin{bmatrix} \mathbf{h} \\ \mathbf{0} \end{bmatrix} = \begin{bmatrix} \mathbf{H}_a & \mathbf{H}_u \\ \mathbf{0} & \mathbf{I} \end{bmatrix} \begin{bmatrix} \ddot{\mathbf{q}}_a \\ \ddot{\mathbf{q}}_u \end{bmatrix} + \begin{bmatrix} \mathbf{h} \\ \mathbf{0} \end{bmatrix} = \mathbf{H}'(\mathbf{q})\ddot{\mathbf{q}} + \mathbf{h}'(\mathbf{q}, \dot{\mathbf{q}}) \tag{3.2}$$

where $\mathbf{H}'$ is the $f \times f$ matrix of transformation whose inverse is conditioned upon $\det \mathbf{H}_a \neq 0$. A simple way to express the underactuated system dynamics in the new coordinate set, directly in the resolved form, is just to substitute $\ddot{\mathbf{q}} = \mathbf{M}^{-1}(\mathbf{g} - \mathbf{k} + \mathbf{B}\mathbf{u})$, obtained from Eq. (2.1), into Eq. (3.2), which gives

$$\left.\begin{aligned} \ddot{\mathbf{y}} &= \mathbf{H}\mathbf{M}^{-1}(\mathbf{g} - \mathbf{k}) + \mathbf{h} + \mathbf{H}\mathbf{M}^{-1}\mathbf{B}\mathbf{u} \\ \ddot{\mathbf{q}}_u &= \begin{bmatrix} \mathbf{0} \,\vdots\, \mathbf{I} \end{bmatrix}\mathbf{M}^{-1}(\mathbf{g} - \mathbf{k}) + \begin{bmatrix} \mathbf{0} \,\vdots\, \mathbf{I} \end{bmatrix}\mathbf{M}^{-1}\mathbf{B}\mathbf{u} \end{aligned}\right\} \Longleftrightarrow \left\{\begin{aligned} \ddot{\mathbf{y}} &= \mathbf{f}_y(\mathbf{q}, \dot{\mathbf{q}}) + \mathbf{Y}(\mathbf{q})\mathbf{u} \\ \ddot{\mathbf{q}}_u &= \mathbf{f}_q(\mathbf{q}, \dot{\mathbf{q}}) + \mathbf{Q}(\mathbf{q})\mathbf{u} \end{aligned}\right. \tag{3.3}$$

where $\mathbf{f}_y = \mathbf{H}\mathbf{M}^{-1}(\mathbf{g} - \mathbf{k}) + \mathbf{h}$ and $\mathbf{f}_q = [\mathbf{0} \,\vdots\, \mathbf{I}]\mathbf{M}^{-1}(\mathbf{g} - \mathbf{k})$ are m and $(f - m)$ dimensional vectors, respectively, $\mathbf{Y} = \mathbf{H}\mathbf{M}^{-1}\mathbf{B}$ is the $m \times m$ matrix introduced above, and the matrix $\mathbf{Q} = [\mathbf{0} \,\vdots\, \mathbf{I}]\mathbf{M}^{-1}\mathbf{B}$ is of dimension $(f - m) \times m$. For the case of orthogonal realization of servo-constraints, $\det \mathbf{Y} \neq 0$, the first relationship of Eq. (3.3) explicitly relates $\mathbf{u}$ and $\ddot{\mathbf{y}}$. The feedforward control $\mathbf{u}(t)$ required for exact reproduction of $\tilde{\ddot{\mathbf{y}}}(t)$ can then effectively be computed as

$$\mathbf{u}(t, \mathbf{q}, \dot{\mathbf{q}}) = \mathbf{Y}^{-1}(\tilde{\ddot{\mathbf{y}}} - \mathbf{f}_y) \tag{3.4}$$

A feedback-enhanced controller can be designed by applying $\ddot{\mathbf{y}}_{stab} = \tilde{\ddot{\mathbf{y}}} + \boldsymbol{\alpha}(\tilde{\dot{\mathbf{y}}} - \dot{\mathbf{y}}) + \boldsymbol{\beta}(\tilde{\mathbf{y}} - \mathbf{y})$ instead of $\tilde{\ddot{\mathbf{y}}}$, where $\boldsymbol{\alpha}$ and $\boldsymbol{\beta}$ are the diagonal matrices of gain values, and $\mathbf{y}$ and $\dot{\mathbf{y}}$ are respectively the actual output and its time-derivative. A scheme of manipulator control, based on explicit output-input relationship (3.4), is illustrated in Fig. 1.

The symbolic representation of Eq. (3.3) shows that the servo-constraint problem at hand can be viewed as an (algebraic) input-output normal form of Eq. $(3.3)_1$, resulting in the feedforward control law of Eq. (3.4) and an ODE representation for the internal dynamics, Eq. $(3.3)_2$. Since the control required for the orthogonal realization of servo-constraints and the internal dynamics evolution are mutually dependent, of critical importance for the control strategy is therefore that the internal dynamics remains bounded. The case of orthogonal realization of servo-constraints for an underactuated system is therefore not trivial; see also Seifried (2012a) and Seifried and Blajer (2013), where the problem is given a more detailed consideration.
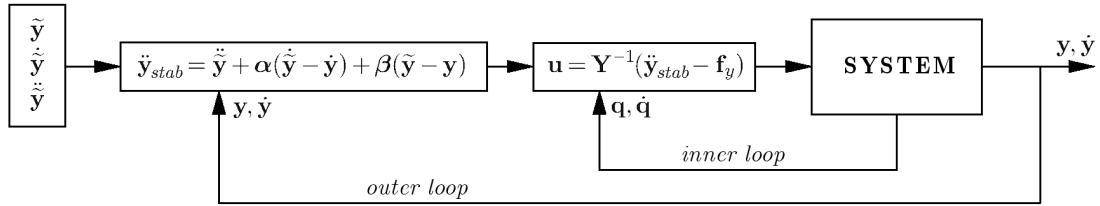
Fig. 1. Structure of control with inner and outer loops, based on explicit output-input relationship (3.4)

The dynamic equations in the form of Eq. (3.3) can also serve as a basis for a DAE set of the governing equations. Since the dynamic equations that govern $\ddot{\mathbf{q}}' = [\ddot{\mathbf{y}}^{\mathrm{T}} \quad \ddot{\mathbf{q}}_u^{\mathrm{T}}]^{\mathrm{T}}$ depend on the states $\mathbf{q}$ and $\dot{\mathbf{q}}$, the servo-constraint equations at the position and velocity level must be appended, and the involvement of the servo-constraint equations at the acceleration level is equivalent to using $\ddot{\mathbf{y}} = \ddot{\tilde{\mathbf{y}}}(t)$ in Eq. (3.3)$_2$. The arising set of $2f + m$ DAEs in $\mathbf{q}$, $\mathbf{v}$ and $\mathbf{u}$ is the following

$$\left.\begin{aligned}
\dot{\mathbf{q}}_u &= \mathbf{v}_u \\
\dot{\mathbf{v}}_u &= \mathbf{f}_q(\mathbf{q}, \dot{\mathbf{q}}) + \mathbf{Q}(\mathbf{q})\mathbf{u} \\
\mathbf{0} &= \mathbf{f}_y(\mathbf{q}, \dot{\mathbf{q}}) + \mathbf{Y}(\mathbf{q})\mathbf{u} - \ddot{\tilde{\mathbf{y}}}(t) \\
\mathbf{0} &= \mathbf{H}(\mathbf{q})\dot{\mathbf{q}} - \dot{\tilde{\mathbf{y}}}(t) \\
\mathbf{0} &= \mathbf{\Phi}(\mathbf{q}) - \tilde{\mathbf{y}}(t)
\end{aligned}\right\} \iff \left\{\begin{aligned}
\dot{\mathbf{q}}_u &= \mathbf{v}_u \\
\dot{\mathbf{v}}_u &= \mathbf{b}(\mathbf{q}, \dot{\mathbf{q}}, \mathbf{u}) \\
\mathbf{0} &= \boldsymbol{\eta}(\mathbf{q}, \dot{\mathbf{q}}, \mathbf{u}, t) \\
\mathbf{0} &= \boldsymbol{\gamma}(\mathbf{q}, \dot{\mathbf{q}}, t) \\
\mathbf{0} &= \boldsymbol{\varphi}(\mathbf{q}, t)
\end{aligned}\right. \tag{3.5}$$

The design of control of an underactuated system in the prescribed trajectory motion can be based on the solution to the DAEs. A simple numerical code for this solution, previously implemented by Blajer and Kołodziejczyk (2007), can be based on the Euler backward differentiation scheme in which the time derivatives of the variables are approximated with their backward differences with respect to the integration time step Δt. Given $\mathbf{q}_n$ and $\mathbf{v}_n$ at time t_n ($\mathbf{u}_n$ are not required), the values $\mathbf{q}_{n+1}$, $\mathbf{v}_{n+1}$ and $\mathbf{u}_{n+1}$ at time $t_{n+1} = t_n + \Delta t$ are obtained as a solution to the following nonlinear equations

$$\begin{aligned}
(\mathbf{q}_u)_{n+1} - (\mathbf{q}_u)_n - \Delta t(\mathbf{v}_u)_{n+1} &= \mathbf{0} \\
(\mathbf{v}_u)_{n+1} - (\mathbf{v}_u)_n - \Delta t\mathbf{b}(\mathbf{q}_{n+1}, \mathbf{v}_{n+1}, \mathbf{u}_{n+1}) &= \mathbf{0} \\
\boldsymbol{\eta}(\mathbf{q}_{n+1}, \mathbf{v}_{n+1}, \mathbf{u}_{n+1}, t_{n+1}) &= \mathbf{0} \\
\boldsymbol{\gamma}(\mathbf{q}_{n+1}, \mathbf{v}_{n+1}, t_{n+1}) &= \mathbf{0} \\
\boldsymbol{\varphi}(\mathbf{q}_{n+1}, t_{n+1}) &= \mathbf{0}
\end{aligned} \tag{3.6}$$

In this way, the solutions are advanced from t_n to t_{n+1}, and the rough computational scheme is of acceptable accuracy only for on appropriately small Δt. The accuracy can be improved by applying higher-order backward difference approximations or other specialized DAE solvers (Ascher and Petzold, 1998). A scheme of manipulator control, based on the DAE formulation, is illustrated in Fig. 2.
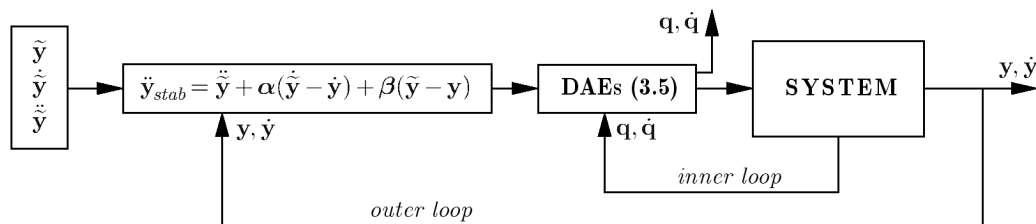

Fig. 2. Structure of control based on DAE formulation (3.5)

4. Case study illustration

Consider a 3-degree-of-freedom planar manipulator seen in Fig. 3a, with the actuated joints O_1 and O_2, and the passive joint A with a spring-damper combination. The vanishing torque of the torsional spring is achieved for $\theta_3 = \theta_2$, and the arm moves in the horizontal plane perpendicular to the direction of gravity. Defined $\mathbf{q} = [\theta_1, \theta_2, \theta_3]^{\mathrm{T}}$ and $\mathbf{u} = [\tau_1, \tau_2]^{\mathrm{T}}$, the components of the arm dynamic equations introduced in Eq. (2.1) are defined by

$$
\begin{aligned}
M_{1,1} &= J_{C1} + m_1 s_1^2 + (m_2 + m_3 + m_4) l_1^2 \\
M_{1,2} &= M_{2,1} = [m_2 s_2 + (m_3 + m_4) l_2] l_1 \cos(\theta_2 - \theta_1) \\
M_{1,3} &= M_{3,1} = (m_3 s_3 + m_4 l_3) l_1 \cos(\theta_3 - \theta_1) \\
M_{2,2} &= J_{C2} + m_2 s_2^2 + (m_3 + m_4) l_2^2 \\
M_{2,3} &= M_{3,2} = (m_3 s_3 + m_4 l_3) l_2 \cos(\theta_3 - \theta_2) \\
M_{3,3} &= J_{C3} + m_3 s_3^2 + m_4 l_3^2
\end{aligned}
\tag{4.1}
$$

and

$$
\mathbf{k} = \begin{bmatrix} -[m_2 s_2 + (m_3 + m_4) l_2] l_1 \dot{\theta}_2^2 \sin(\theta_2 - \theta_1) - (m_3 s_3 + m_4 l_3) l_1 \dot{\theta}_3^2 \sin(\theta_3 - \theta_1) \\ [m_2 s_2 + (m_3 + m_4) l_2] l_1 \dot{\theta}_1^2 \sin(\theta_2 - \theta_1) - (m_3 s_3 + m_4 l_3) l_2 \dot{\theta}_3^2 \sin(\theta_3 - \theta_2) \\ (m_3 s_3 + m_4 l_3) l_1 \dot{\theta}_1^2 \sin(\theta_3 - \theta_1) + (m_3 s_3 + m_4 l_3) l_2 \dot{\theta}_2^2 \sin(\theta_3 - \theta_2) \end{bmatrix}
$$

$$
\mathbf{g} = \begin{bmatrix} 0 \\ c(\theta_3 - \theta_2) + d(\dot{\theta}_3 - \dot{\theta}_2) \\ -c(\theta_3 - \theta_2) - d(\dot{\theta}_3 - \dot{\theta}_2) \end{bmatrix} \qquad \mathbf{B} = \begin{bmatrix} 1 & -1 \\ 0 & 1 \\ 0 & 0 \end{bmatrix}
\tag{4.2}
$$

where m_i, J_{Ci}, l_i and s_i ($i = 1, 2, 3$) are the respective link masses, central mass moments of inertia, lengths, and locations of the mass center (distances $O_1 C_1$, $O_2 C_2$ and AC_3), m_4 is an additional mass at the top of link 3, and c and d are the spring and damper constants.
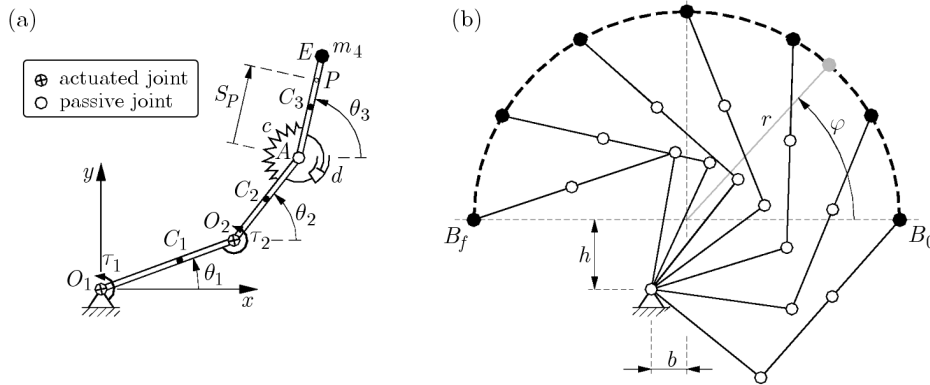

Fig. 3. A planar manipulator arm with two active and one passive joint: (a) the model; (b) illustration of the assigned task for $\theta_3 = \theta_2$

The desired task is to move the end point E along a circle of radius r, from the point B_0 to point B_f on the circle, illustrated in Fig. 3b for the case $\theta_3 = \theta_2$. The maneuver can be accomplished by imposing the following time-specified function of the angle φ (defined in the figure), used previously in Blajer and Kołodziejczyk (2007)

$$
\widetilde{\varphi}(t) = \varphi_0 + \left[126 \left(\frac{t}{T} \right)^5 - 420 \left(\frac{t}{T} \right)^6 + 540 \left(\frac{t}{T} \right)^7 - 315 \left(\frac{t}{T} \right)^8 + 70 \left(\frac{t}{T} \right)^9 \right] (\varphi_f - \varphi_0)
\tag{4.3}
$$

where $\varphi_0 = \widetilde{\varphi}(0)$ and $\varphi_f = \widetilde{\varphi}(T)$ are the initial and final values of φ, and T is the maneuver duration. This is a rest-to-rest maneuver assuring the steady state conditions $\dot{\widetilde{\varphi}}(0) = \dot{\widetilde{\varphi}}(T) = 0$,

$\ddot{\widetilde{\varphi}}(0) = \ddot{\widetilde{\varphi}}(T) = 0$, $\dddot{\widetilde{\varphi}}(0) = \dddot{\widetilde{\varphi}}(T) = 0$ and $\widetilde{\varphi}^{(4)}(0) = \widetilde{\varphi}^{(4)}(T) = 0$. In further simulations, we used then: $\varphi_0 = 0°$, $\varphi_f = 180°$, $l_1 = 0.8$ m, $l_2 = l_3 = 0.6$ m, $r = 1.2$ m, $b = 0.2$ m and $h = 0.4$ m.

For the above task, there is a natural tendency to assign the outputs to the coordinates of the point E, $\widetilde{\mathbf{y}}(t) = [\widetilde{x}_E(t), \widetilde{y}_E(t)]^{\mathrm{T}}$, with $\widetilde{x}_E(t) = b + r\cos(\widetilde{\varphi}(t))$ and $\widetilde{y}_E(t) = h + r\sin(\widetilde{\varphi}(t))$. This output allocation may be improper, however, resulting in an unbounded internal dynamics (Seifried, 2012a,b). The reason for the inappropriateness of the end-effector output assignment can be illustrated with a little simpler example – a rotational arm with one active and one passive joint, seen in Fig. 4a. Let us assume that the arm is in rest in the position seen, and the task is to move the end point E in the y direction, yielding $\ddot{\widetilde{y}}_E > 0$. Intuitively, one can expect a positive (counterclockwise) sense of τ required to initiate the upward motion of the point E. This may not be the case, however. More strictly, the effect of τ on link 2 is an upward reaction R in the joint A (Fig. 4b), which moved to the link mass center C_2 is associated with a couple with a clockwise torque $T = Rs_2$. Assumed link 2 is homogeneous, i.e. $s_2 = l_2/2$ and $J_{C2} = m_2 l_2^2/12$, the acceleration of the point E is then

$$\ddot{y}_E = \frac{R}{m_2} - \frac{Rs_2}{J_{C2}}(l_2 - s_2) = \frac{R}{m_2} - \frac{Rl_2}{2}\frac{12}{m_2 l_2^2}\frac{l_2}{2} = -\frac{2R}{m_2} \tag{4.4}$$

The action of a "positive" τ has thus the opposite effect from what is expected – a "negative" $\ddot{\widetilde{y}}_E$ is produced. A "positive" $\ddot{\widetilde{y}}_E$ will thus require a "negative" τ. This "reverse" control is certainly wrong, and, when continued, will soon lead to collapse of the servo-constraint problem execution. As shown by Seifried (2012a), the inverse simulation control inappropriateness can be overcome by modifying (optimizing) the system parameters, resulting specifically in reducing s_2 and enlarging J_{C2} so that the same senses in the input-output relationship are achieved. Another possibility is reformulation of the desired output $\widetilde{\mathbf{y}}(t)$, applied in the following for the present case study.
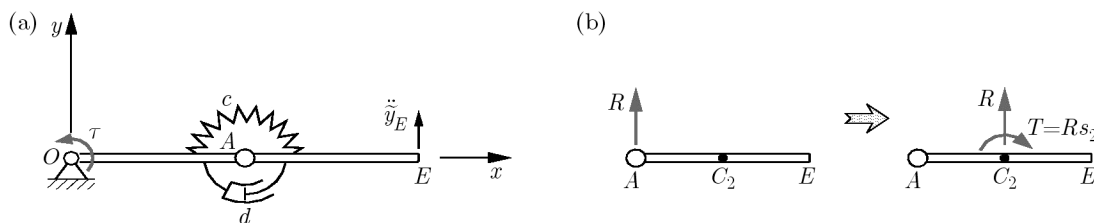

Fig. 4. A rotational arm with one active and one passive joint: (a) the model; (b) illustration of the action of control torque τ on link 2

The described inappropriateness in the output-input inverse model, which relates also the present case study, can be overcome by assigning the outputs to the coordinates of the inner point P instead of the end point E (Fig. 3a), $\mathbf{y} = [x_P, y_P]^{\mathrm{T}}$, and a reasonable choice used in the forthcoming simulations is $P \to C_3$ ($s_P = l_3/2$). The output relationships of Eq. (2.2) are then defined by

$$\mathbf{y} = \begin{bmatrix} x_P \\ y_P \end{bmatrix} = \begin{bmatrix} l_1\cos\theta_1 + l_2\cos\theta_2 + s_P\cos\theta_3 \\ l_1\sin\theta_1 + l_2\sin\theta_2 + s_P\sin\theta_3 \end{bmatrix}$$

$$\mathbf{H} = \begin{bmatrix} -l_1\sin\theta_1 & -l_2\sin\theta_2 & -s_P\sin\theta_3 \\ l_1\cos\theta_1 & l_2\cos\theta_2 & s_P\cos\theta_3 \end{bmatrix} \tag{4.5}$$

$$\mathbf{h} = \begin{bmatrix} -l_1\dot{\theta}_1^2\cos\theta_1 - l_2\dot{\theta}_2^2\cos\theta_2 - s_P\dot{\theta}_3^2\cos\theta_3 \\ -l_1\dot{\theta}_1^2\sin\theta_1 - l_2\dot{\theta}_2^2\sin\theta_2 - s_P\dot{\theta}_3^2\sin\theta_3 \end{bmatrix}$$

The reference trajectories $\widetilde{\mathbf{y}}(t) = [\widetilde{x}_P, \widetilde{y}_P]^{\mathrm{T}} \to \dot{\widetilde{\mathbf{y}}}(t) = [\dot{\widetilde{x}}_P, \dot{\widetilde{y}}_P]^{\mathrm{T}} \to \ddot{\widetilde{\mathbf{y}}}(t) = [\ddot{\widetilde{x}}_P, \ddot{\widetilde{y}}_P]^{\mathrm{T}}$ have been determined from the manipulator inverse kinematics for $\theta_3 = \theta_2$, illustrated in Fig. 5 together with the end point E trajectories. The assumed maneuver duration was $T = 5\,\mathrm{s}$.
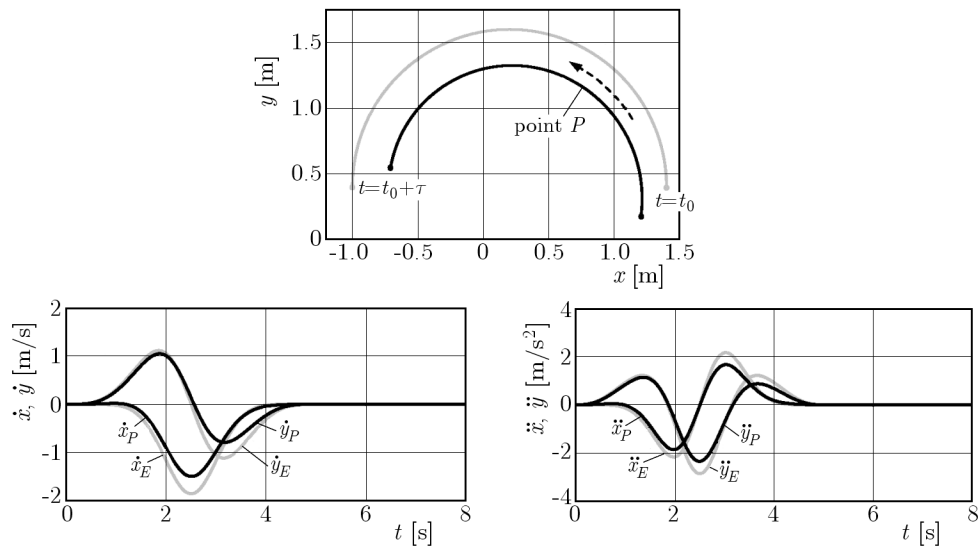

Fig. 5. The reference trajectories for points P (black lines) and E (grey lines)

The results of inverse dynamics simulation for the manipulator arm tracking the specified motion of the point P are illustrated in Fig. 6. In addition to the abovementioned manipulator geometrical parameters and the task specifications, the inertial parameters used in calculations were: $m_1 = 8\mathrm{kg}$, $m_2 = m_3 = 6\,\mathrm{kg}$, $m_4 = 10\,\mathrm{kg}$, $J_{C1} = 0.45\,\mathrm{kg\,m^2}$, $J_{C2} = J_{C3} = 0.2\,\mathrm{kg\,m^2}$, and the stiffness and damping coefficients were $c = 10\,\mathrm{Mm/rad}$ and $d = 2\,\mathrm{Mm\,s/rad}$. The integration time step was $\Delta t = 0.001\,\mathrm{s}$. As seen from the graphs, the internal dynamics is bounded (stabilized), and, due to the assumed damping in the passive joint, the manipulator quickly achieves the final rest position for $t > T = 5\,\mathrm{s}$. Since the specification of the point $P \to C_3$, $\widetilde{\mathbf{y}}(t) = [\widetilde{x}_P(t), \widetilde{y}_P(t)]^{\mathrm{T}}$, the motion of the end point E is affected also by the internal motion evolution. The resulted trajectory and velocity components of the point E are shown in Fig. 7 (black lines), compared to those obtained for $\theta_3 = \theta_2$ (grey lines).
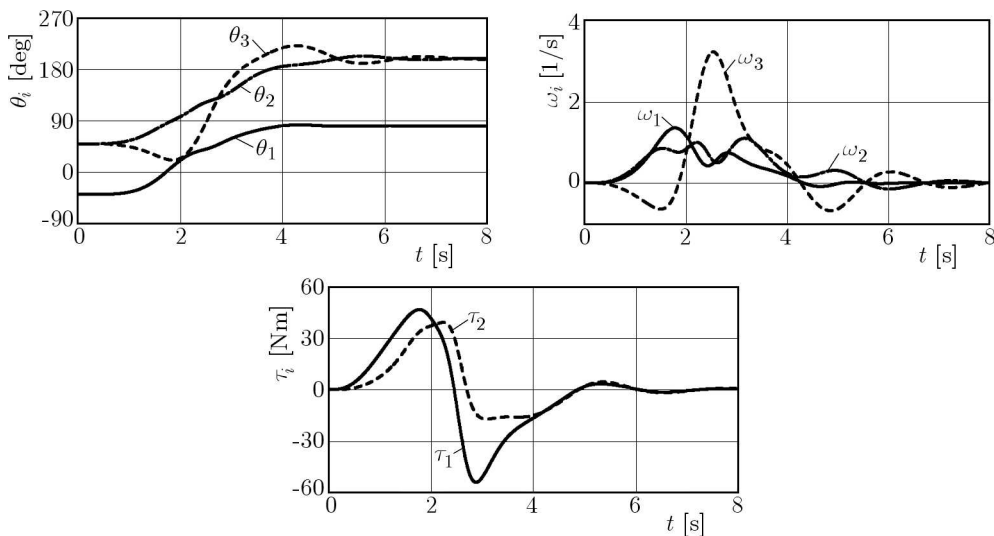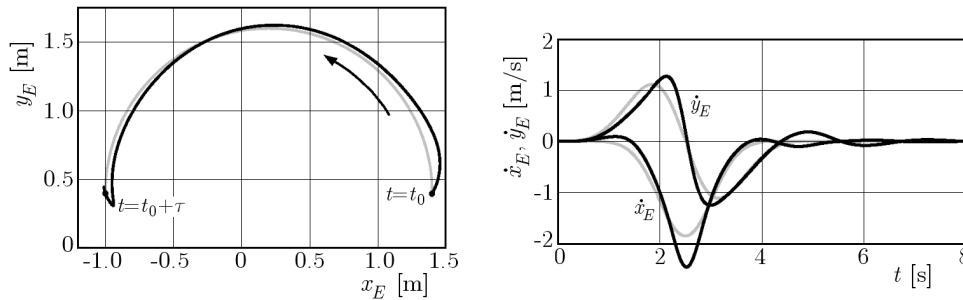

Fig. 6. Simulation of the manipulator motion and control in the prescribed motion

Fig. 7. Motion of the end point E

5. Summary and conclusions

Manipulators with passive joints, studied in this paper, fall into the category of non-flat underactuated systems. A non-ideal orthogonal realization of servo-constraints imposed on the systems is observed, denoting that the inputs can directly regulate the motion specifications. However, besides the output-input inverse dynamics model, exemplified in Eqs. $(3.3)_1$, (3.4) and $(3.5)_3$, an additional internal dynamics arises. The servo-constraint problem becomes thus a dynamical model, with the internal dynamics which may be bounded (stable) or unbounded (unstable). Meaningful solutions to the servo-constraint problem require therefore a careful analysis related both to the design of the underactuated manipulator and to the imposed motion specifications.

For the case study analyzed in the paper, choosing the end-effector position coordinates as outputs, and then specifying them in time to formulate servo-constraints on the system, is not a good practice. While the orthogonal realization of the servo-constraints is maintained and the inverse dynamics control can explicitly be determined, the assisted internal dynamics (affected by the required control) is unbounded, and the solution leads to collapse. It was shown by Seifried (2012a) that the situation can be improved by modifying/optimizing the design parameters of the underactuated system, usually the geometric dimensions and mass distribution. The other possibility, motivated in this contribution, is to choose some appropriate outputs. Regulating some inner point position, instead of the end-effector position, is recommended. The servo-constraint problem execution becomes then stable without any modification to the original system design. The sacrifice is that, whereas the exact tracking of the inner point (specified) trajectory is assured, the end-effector motion is also affected by the internal dynamics. The end-effector trajectory tracking is then realized with a limited accuracy. The situation can be improved by enlarging (or additionally adding) the damping in the system, and, evidently, for large stiffness in the passive joint the solution becomes similar to that obtained for a "rigid" manipulator (with the passive joint jammed). Finally, it may be worth noting that the stabilization of the servo-constraint problem execution with limited accuracy was also discussed in e.g. Seifried (2011,b) and Kovács and Bencsik (2012), where a linearly combined output instead of the end-effector position was used as the reference trajectory, which is somewhat equivalent to the regulating of the inner point position used in the present paper.

References

1. ASCHER U.M., PETZOLD L.R., 1998, *Computer Methods for Ordinary Differential Equations and Differential–Algebraic Equations*, SIAM, Philadelphia

2. BAJODAH A.H., HODGES D.H., CHEN Y.-H., 2005, Inverse dynamics of servo-constraints based on the generalized inverse, *Nonlinear Dynamics*, **39**, 1/2, 179-196

3. Benosman M., Le Vey G., 2004, Control of flexible manipulators: a survey, *Robotica*, **22**, 5, 533-545

4. Blajer W., Kołodziejczyk K., 2007, Control of underactuated mechanical systems with servoconstraints, *Nonlinear Dynamics*, **50**, 4, 781-791

5. Blajer W., Kołodziejczyk K., 2008, Modeling of underactuated mechanical systems in partly specified motion, *Journal of Theoretical and Applied Mechanics*, **46**, 2, 383-394

6. Blajer W., Seifried R., 2012, From orthogonal to tangential control of underactuated mechanical systems in partly specified motion – a cases study illustration, *International Journal of Applied Mechanics and Engineering*, **17**, 3, 689-706

7. De Luca A., Oriolo G., 2002, Trajectory planning and control for planar robots with passive last joint, *The International Journal of Robotics Research*, **21**, 5/6, 575-590

8. Fantoni I., Lozano R., 2002, *Non-linear Control for Underactuated Mechanical Systems*, Springer, London

9. Fliess M., Lévine J., Martin P., Rouchon P., 1995, Flatness and defect of nonlinear systems: introductory theory and examples, *International Journal of Control*, **61**, 6, 1327-1361

10. Kirgetov V.I., 1967, The motion of controlled mechanical systems with prescribed constraints (servoconstraints), *Journal of Applied Mathematics and Mechanics*, **31**, 3, 433-466

11. Kovács L.L., Bencsik L., 2012, Stability case study of the ACROBOTER underactuated service robot, *Theoretical and Applied Mechanics Letters*, **2**, 4, paper ID: 043004 (7 pages)

12. Paul R.P., 1981, *Robot Manipulators: Mathematics, Programming, and Control*, MIT Press, Cambridge, MA

13. R. Seifried R., 2011, Optimization-based design of minimum phase underactuated multibody systems, [In:] *Multibody Dynamics: Computational Methods and Applications*, Arczewski K., Blajer W., Frączek J., Wojtyra M. (Eds.), Springer, Dordrecht, 261-282

14. Seifried R., 2012a, Integrated mechanical and control design of underactuated multibody systems, *Nonlinear Dynamics*, **67**, 2, 1539-1557

15. Seifried R., 2012b, Two approaches for feedforward control and optimal design of underactuated multibody systems, *Multibody System Dynamics*, **27**, 1, 75-93

16. Seifried R., Blajer W., 2013, Analysis of servo-constraint problems for underactuated multibody systems, *Mechanical Sciences*, **4**, 1, 113-129

17. Spong M.W., 1987, Modeling and control of elastic joint robots, *Transactions of the ASME, Journal of Dynamic Systems, Measurements, and Control*, **109**, 4, 310-319

18. Spong M.W., 1998, Underactuated mechanical systems, [In:] *Control Problems in Robotics and Automation*, Siciliano B., Valavanis K.P. (Eds.), Springer, London, 135-150